Improving the Prediction of the East Asian Summer Monsoon: New Approaches

KE FAN

Nansen-Zhu International Research Centre, Institute of Atmospheric Physics, and Key Laboratory of Regional Climate-Environment for East Asia, Chinese Academy of Sciences, Beijing, China

YING LIU

Nansen-Zhu International Research Centre, Institute of Atmospheric Physics, Chinese Academy of Sciences, and Graduate University of the Chinese Academy of Sciences, Beijing, China

HUOPO CHEN

Nansen-Zhu International Research Centre, Institute of Atmospheric Physics, Chinese Academy of Sciences, Beijing, China

(Manuscript received 5 September 2011, in final form 28 March 2012)

ABSTRACT

East Asian summer monsoon (EASM) prediction is difficult because of the summer monsoon's weak and unstable linkage with El Niño–Southern Oscillation (ENSO) interdecadal variability and its complicated association with high-latitude processes. Two statistical prediction schemes were developed to include the interannual increment approach to improve the seasonal prediction of the EASM's strength. The schemes were applied to three models [i.e., the Centre National de Recherches Météorologiques (CNRM), the Met Office (UKMO), and the European Centre for Medium-Range Weather Forecasts (ECMWF)] and the Multimodel Ensemble (MME) from the Development of a European Multimodel Ensemble System for Seasonal-to-Interannual Prediction (DEMETER) results for 1961–2001. The inability of the three dynamical models to reproduce the weakened East Asian monsoon at the end of the 1970s leads to low prediction ability for the interannual variability of the EASM. Therefore, the interannual increment prediction approach was applied to overcome this issue. Scheme I contained the EASM in the form of year-to-year increments as a predictor that is derived from the direct outputs of the models. Scheme II contained two predictors: both the EASM and also the western North Pacific circulation in the form of year-to-year increments. Both the cross-validation test and the independent hindcast experiments showed that the two prediction schemes have a much better prediction ability for the EASM than does the original scheme. This study provides an efficient approach for predicting the EASM.

1. Introduction

The interannual and decadal variability of the Asian summer monsoon plays an important role in the variability of precipitation and temperature across Asia. Seasonal prediction of the Asian summer monsoon is of great value to Asian countries for agriculture, water resource management, and flood and drought disaster reduction. However, the skillful prediction of monsoons, particularly those over East Asia, is difficult because of the monsoons' weak and unstable linkage with ENSO (Wang 2002), interdecadal variability (Wang 2001; Zhu et al. 2011), and complicated association with high-latitude processes (Fan and Wang 2006; Wang and Fan 2005; Zhou and Wang 2006).

The East Asian summer monsoon (EASM) is a component of the Asian summer monsoon, whose major area is 20°–40°N × 110°–125°E. The EASM circulation system includes the western Pacific subtropical high, the cross-equatorial cross flow in the lower atmosphere over the South China Sea, the monsoon trough, and the mei-yu front (Tao and Chen 1987; Ding and Chan 2005). With the seasonal march of the EASM, the EASM rain belt moves northward between the spring and summer and

Corresponding author address: Ke Fan, Nansen-Zhu International Research Centre, Institute of Atmospheric Physics, Chinese Academy of Sciences, Beijing Chaoyang District, Huayanli 40, Beijing 100029, China.
E-mail: fanke@mail.iap.ac.cn

DOI: 10.1175/WAF-D-11-00092.1

then retreats south in the late summer and autumn. Meanwhile, the domain of the South Asia monsoon, which is considered to be another component of the Asian summer monsoon, covers the tropical area that consists mainly of the Mascarene high, the Somali jet, and the westerly wind in the region. The East Asian summer monsoon undergoes high-amplitude interannual and interdecadal variability. The Asian monsoon circulation became weakened after the end of the 1970s, with more rainfall over the Yangtze River valley and less rainfall over northern China (Wang 2001; Wang 2002; Zhou and Wang 2006). Another new decadal shift of the East Asian monsoon rainfall pattern may have appeared approximately at the end of 1999, with the occurrence of abundant rainfall over the Huanghuai River valley and deficient rainfall over the Yangtze River valley (Zhu et al. 2011).

Dynamical seasonal prediction has mainly been performed by tier-one and -two prediction systems in most operation centers. In the tier-two systems, the seasonal prediction is performed using only the atmospheric general climate model (AGCM) with the prescribed SST boundary condition. The tier-one system uses a coupled GCM, which includes an interacting physics relation between the atmosphere and the ocean. The Development of a European Multimodel Ensemble System for Seasonal-to-Interannual Prediction (DEMETER) project was conceived to produce a series of 6-month multimodel ensemble hindcasts by running a number of state-of-the-art global coupled ocean–atmosphere models on a single supercomputer with common archiving and diagnostic software (Palmer et al. 2004). The multimodel superensemble prediction has been used in climate prediction to produce more reliable probability forecasts (Krishnamurti et al. 1999). However, these GCMs show poor performance over the East Asian monsoon area (Kang et al. 2002; Wang and Fan 2009; Yang et al. 2008). Subsequently, so-called downscaling techniques have subsequently emerged as a means of bridging the gap between what climate models are currently able to provide and what impact assessors require. Conventional downscaling ought to create high-resolution forecasts based on dynamical or statistical methods (Wilby and Wigley 1997). The dynamical downscaling involves nesting the general circulation models (GCMs) with increasingly higher spatial resolution (Gao et al. 2006; Ju et al. 2007).

The large-scale fields from the observations or dynamical results are normally referred to as the predictors, and the local climate variables are known as the predictands. The latter approach relies on historical studies of the relationship between large-scale climatic anomalies and local climate fluctuations; this approach implicitly assumes that past relationships also hold in the future. There are numerous ways to develop empirical models (Wilby et al. 1998; Wang et al. 2000; Wang and Fan 2009; Lang and Wang 2010; Liu et al. 2011) and apply these to the dynamical model results to obtain local climate predictions.

An interannual increment prediction approach was proposed by Fan et al. (2008), which showed an improved prediction ability for seasonal climate prediction of the summer rainfall in eastern China, temperature in northeast China, and the activity of the western North Pacific (WNP) typhoons and the Atlantic hurricanes (Fan et al. 2008; Fan et al. 2009; Fan and Wang 2009; Fan 2010, Wang et al. 2010). This approach utilized the year-to-year increment (or DY of a variable, i.e., a difference in the variable between the current year and the previous year) as the predictand, and the predictors are all in the form of the interannual increment. First, the DY of a variable is predicted; subsequently, the original variable is obtained by adding the predicted DY of the variable to the observed value from the previous year. The rationality of this approach originated from the tropospheric biennial oscillation (TBO) feature of climate variables, such as the monsoon index and rainfall over East Asia, such that a variable in the interannual increment may capture more of the TBO feature and the variable's decadal variability than a variable in the original approach. The advantages of the DY method include the following. 1) The interannual increment of a variable reflects the TBO and amplifies the prediction signal and makes good use of the climate observations from the previous year. 2) The DY method can capture the interannual and decadal variability of the climate, as it is difficult to capture the decadal variability of the climate for statistical or dynamical models. Thus, this interannual increment prediction approach shows a better fit in hindcasting the summer rainfall over the Yangtze River valley and central northern China, as well as the temperature over northeast China (Fan et al. 2008; Fan et al. 2009; Fan 2009).

The strength of the EASM indicates the EASM circulation, which is closely related to summer rainfall patterns in China. Usually, an enhanced EASM tends to be linked with greater than normal rainfall over northern China and lower than normal rainfall over southern China. Therefore, seasonal prediction of an index of the EASM is as important as that of EASM summer precipitation in China (Fig. 1a). Considering the limited seasonal prediction ability for the EASM in existing dynamical and statistical models, we will attempt to apply the interannual increment prediction approach to the hindcasts of the DEMETER model results to develop new statistical prediction schemes for the strength of the EASM.

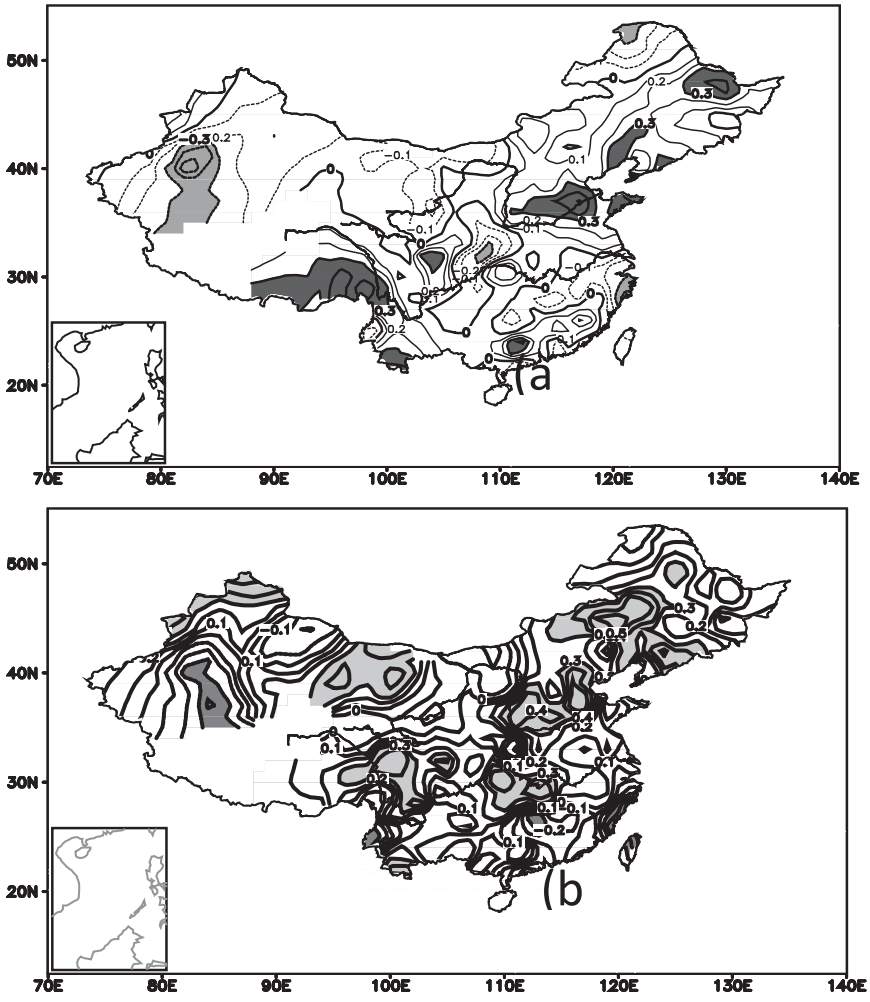

FIG. 1. The correlation coefficient between the EASMI and summer precipitation at 160 stations in China during the 1961–2001 period in (top) the original form and (bottom) the DY form; the shaded areas meet the 95% significance level.

2. Method and dataset

The models used in the DEMETER project were those of the Centre National de Recherches Météorologiques (CNRM), the Met Office (UKMO), and the European Centre for Medium-Range Weather Forecasts (ECMWF). The three models (CNRM, UKMO, and ECMWF) have long hindcasts that covered the same period between 1960 and 2001 (42 yr), starting on 1 May. Each hindcast was integrated for 6 months and comprised an ensemble of nine members. The Multimodels Ensemble (MME) denoted the average of the hindcasts of the UKMO, ECMWF, and CNRM.

The monthly atmospheric reanalysis of the National Centers for Environmental Prediction and the National Center for Atmospheric Research, with a resolution of 2.5° × 2.5°, was used for the atmosphere circulation analyses. The monthly rainfall dataset from 160 stations in China was provided by the Chinese Meteorological Administration.

Following the findings of Wang (2000), the index of the EASM was defined as the zonal and meridional wind departure that was averaged across an area (20°–40°N, 110°–125°E) in June–August (JJA), which represented the strength of the EASM and the pattern of any precipitation anomaly related to the EASM.

The interannual increment prediction approach was applied to develop the prediction schemes. First, the DY of a variable indicates the variable of the current year minus that of the previous year. For example, the DY of the EASM in 1999 is equal to the DY of the EASM in 1999 minus that of 1998 [i.e., DY (1999) = DY (1999) – DY (1998)]. Second, a statistical prediction scheme for the DY of the EASM was established by the multilinear

TABLE 1. The validation of the direct outputs of the models (CNRM, UKMO, ECMWF, and MME) in the hindcasts for the EASM (DY of EASM), measured with the TCC and RMSE. Boldface values indicate results greater than the 95% significance level.

	1961–2001 TCC of EASM (DY of EASM)	1961–79 TCC of EASM (DY of EASM)	1980–2001 TCC of EASM (DY of EASM)	1961–2001 RMSE
CNRM	0.12 **(0.43)**	−0.32 (−0.48)	**0.67 (0.74)**	1.32
UKMO	0.15 **(0.49)**	−0.0002 (0.33)	**0.39 (0.59)**	1.29
ECMWF	0.71 **(0.5)**	0.64 (0.29)	**0.6 (0.63)**	0.73
MME	0.61 **(0.63)**	0.69 (0.29)	**0.69 (0.78)**	0.86

regression method, and the EASM in the original form was obtained by adding the DY of the EASM to the EASM of the previous year.

Both the cross validation for 1961–2001 (41 yr) and the independent hindcasts for the period 1986–2001 (16 yr) were performed to verify the capability of the new approaches on the EASM prediction. The cross validation may be applied by removing each year (along with the previous year from which the year-to-year increment was calculated) from the training set and generating a new set of coefficients based on the retained years. The process was repeated to generate blind forecasts for each year of the entire dataset.

In the independent hindcasts for 1986–2001 (16 yr), not only was the forecast year removed, but all of the future years were also removed. In that way, we had many years of real forecasting. For example, the 1965–85 dataset was used to forecast the year 1986; similarly, the 1965–86 dataset was used to forecast the year 1987, and so on.

3. Atmospheric circulations associated with the EASM and prediction skills in DEMETER models

The EASM index (EASMI) proposed by Wang (2000) represents the precipitation and low-level atmospheric thermal contrast between the East Asian continent and the western Pacific. The enhanced (weakened) EASM indicates the abundant (deficit) rainfall over northern China and deficient rainfall over the Yangtze River valley, along with the negative (positive) sea level pressure anomaly over the East Asian continent (western Pacific) (Wang 2000) (Fig. 1a). The correlation between the DY of the EASM and the DY of precipitation has similar features to those in the original form (Fig. 1b), with larger correlation coefficients. Based on the EASM index, Wang (2001) found that the strength of the EASM weakened after the end of the 1970s. He also noted that the African–Asian monsoon circulation pattern had become weaker and that the trade wind over the tropical eastern Pacific also became weaker after this shift. In addition, this signal was found in the summer precipitation across China.

The time correlation coefficient (TCC) between the prediction and the observations, as well as the root-mean-square error (RMSE), were used to evaluate the model skills. The TCCs of the EASM for the period 1961–2001 (41 yr) for the CNRM, UKMO, ECMWF, and MME were 0.12, 0.15, 0.71, and 0.61, respectively. Meanwhile, for 1961–2000, the RMSEs for the CNRM, UKMO, ECMWF, and MME were 1.32, 1.29, 0.73, and 0.86, respectively, which were all close to the standard variance of the observed EASM of 1.0 (Table 1). Therefore, the CNRM and UKMO models had no prediction ability for the EASM. The ECMWF model had the best prediction ability, with the smallest RMSE among the models. What are the reasons for the low prediction abilities for the EASM in the models?

First, we depicted the interannual variability of the EASM for the CNRM, UKMO, ECMWF, and MME simulations as well as the observations for the period 1961–2001 (Fig. 2). The observations of the EASM

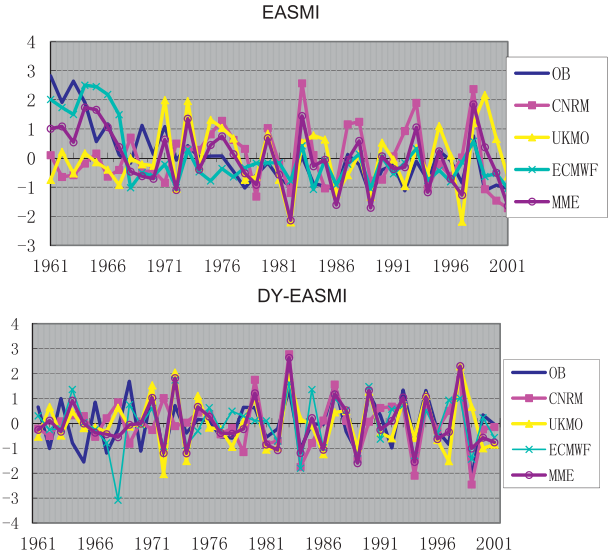

FIG. 2. The 1961–2001 time series of (top) the simulated EASMI and (bottom) the DY of the EASMI for CNRM (red), UKMO (yellow), ECMWF (green), MME (purple), and the observed EASMI (blue).

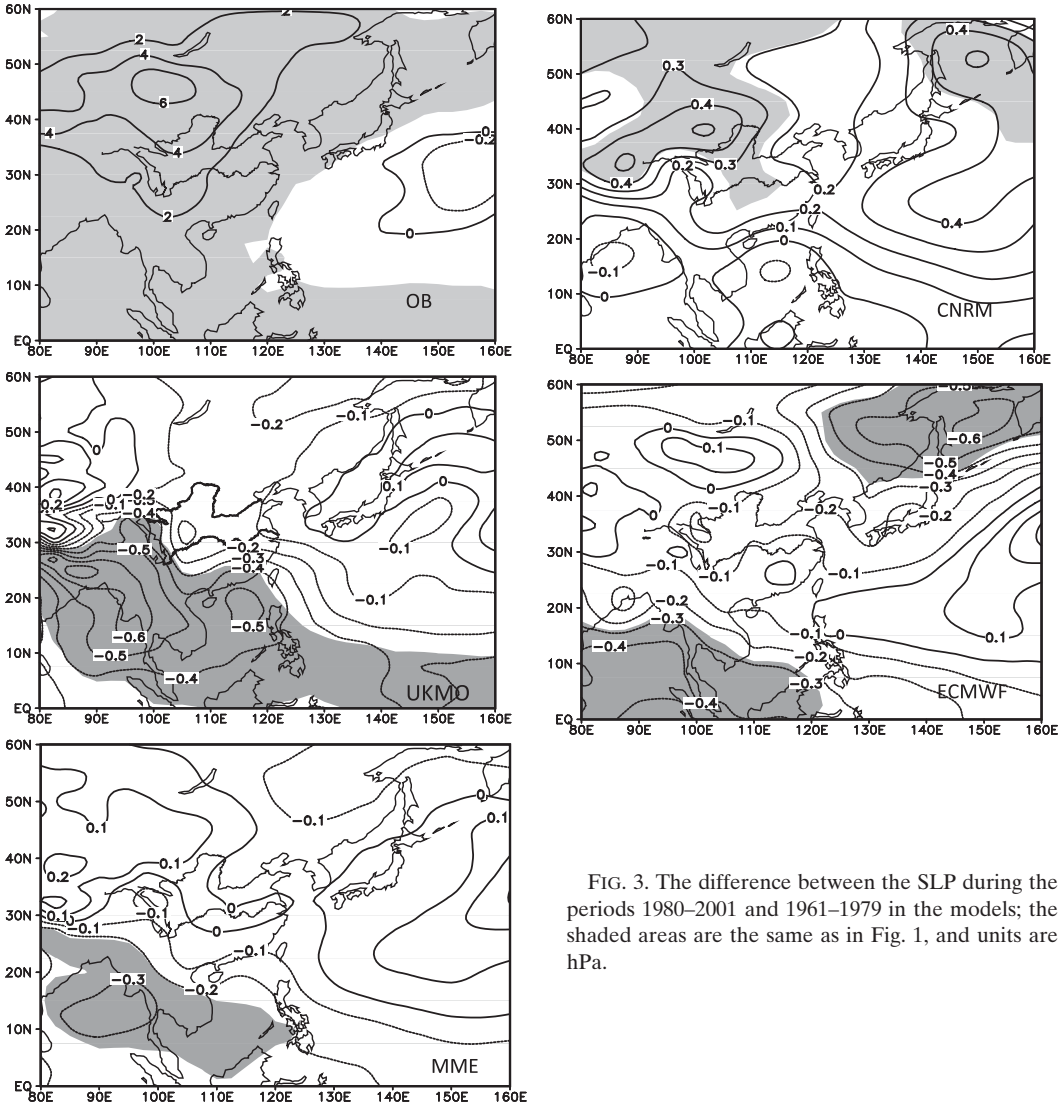

FIG. 3. The difference between the SLP during the periods 1980–2001 and 1961–1979 in the models; the shaded areas are the same as in Fig. 1, and units are hPa.

exhibited a distinct interdecadal variability in 1977, which was consistent with the findings of Wang (2001). Clearly, the ECMWF model was able to reproduce the decadal variability of the EASM, while both the CNRM and UKMO simulations were unable to capture the change. Therefore, the models' inability (CNRM and UKMO) to capture the interdecadal variability may be primarily responsible for the low ability to predict the EASM. To demonstrate this speculation, we examined the TCCs of the EASM for 1961–79 (19 yr) as well as 1980–2001 (22 yr) (Table 1). For the period 1961–79, the TCCs of the EASM for the CNRM, UKMO, ECMWF, and MME were −0.32, −0.002, 0.64, and 0.69, respectively, illustrating that CNRM and UKMO had no prediction ability. For the period 1980–2001, the TCC of the EASM for the CNRM, UKMO, ECMWF, and MME models were 0.67, 0.39, 0.6, and 0.69, respectively, exceeding the significance level of 95%. To further identify the reasons for the low prediction ability for the EASM, we explored the prediction ability for the atmospheric circulations associated with the decadal shift of the EASM. The differences in the sea level pressures (SLPs) between the two periods (1980–2001 and 1961–79) are presented in Fig. 3. After the end of the 1970s, the thermal contrast between the East Asian continent and the western Pacific weakened concurrently with the positive SLP anomaly in the tropics and Eurasia as well as the negative SLP anomaly over the western Pacific. At the same time, the meridional pattern of SLP anomaly between the two periods, with a positive SLP anomaly with large (small) values over Mongolia (southern China). It seems that both land–sea thermal contrasts and the meridional pattern of the SLP anomaly might have played a role in

the weakened EASM at the end of the 1970s. CNRM had a large bias over the North Pacific with the positive SLP anomaly, although it reproduced the positive change over the East Asian continent for the period 1980–2001. UKMO underestimated both the SLP anomaly changes over the East Asian continent and the northern Pacific for the period 1980–2001. Therefore, both the CNRM and UKMO models were unable to present the weakened land–sea thermal contrast at the end of the 1970s. The ECMWF and the MME models reproduce the meridional pattern of the SLP anomaly with a positive SLP anomaly over Mongolia and a negative SLP anomaly over the Yangtze River valley; therefore, the meridional pattern of the SLP anomaly between the two periods might be the cause of the weakening EASM in the ECMWF and the MME results. Correspondingly, in contrast to the period 1961–79, the southerly cyclone over East Asia (i.e., the anticyclone anomaly with a northeastern anomaly) prevailing over eastern China at 850 hPa became weaker (stronger) for the period 1980–2001 (Fig. 4a). However, both the CNRM and the UKMO models were unable to simulate the anticyclone anomaly with the northeastern anomaly (Figs. 4b,c). Meanwhile, the ECMWF and MME simulations underestimated the magnitude of the northeastern anomaly along the East Asian coast (Figs. 4d,e). Therefore, the inaccurate prediction of the difference in the circulation patterns between the two periods led to the poor performance of the models in the prediction of the EASM.

4. The interannual increment prediction approach for the EASM

a. Atmospheric circulations associated with the EASM in the form of year-to-year increments

The DY of a variable that might capture the TBO feature of the variable and produce an amplified signal may facilitate the capture or identification of the marginal changes in the underlying variables. Notably, the approach may capture the trend of the variable by the accumulation of its year-to-year increments (Fan et al. 2008, 2009). We depicted the time series of the DY of the EASM during the period 1961–2001 for the models and MME compared with the observed values (Fig. 2b). As shown in Fig. 2b, the EASM exhibited a remarkable feature of the TBO, with a stronger EASM in the previous year followed by a weaker EASM in the next year, supporting the hypothesis for the rationality of an interannual increment prediction approach. All of the models (ECMWF, CNRM, UKMO, and MME) showed good performance in predicting the DY of the EASM. For the period 1961–2001, the TCCs of the EASM (DY of the EASM) for the CNRM, UKMO, ECMWF, and MME model were 0.12 (0.43), 0.15 (0.49), 0.71 (0.5), and 0.61 (0.63), respectively, with all of the models above the 95% significance level. The TCCs of the DY of the EASM for the period 1961–79 (1980–2001) for CNRM, UKMO, ECMWF, and MME were 0.29 (0.78), −0.48 (0.74), 0.33 (0.59), and 0.29 (0.78), respectively (Table 1). Obviously, the prediction ability for the DY of the EASM was much better than for the EASM in the original form for all of the models during two periods. However, ECMWF did not show as good of a predictive ability for the DY of the EASM as for the EASM for the entire 1961–2001 period.

It is difficult to capture the decadal climate variability for statistical or dynamical models, which results in low prediction ability. Initialization does play a very important role in the decadal and seasonal and interannual climate dynamical predictions (Meehl et al. 2009; Murphy et al. 2010; Keenlyside et al. 2008). Initialization of the ocean, sea ice, snow cover, soil moisture, and other variables should also be considered properly in an ideal dynamical model. However, these historically slowly varying components of climate have been very sparsely observed and some of the data appear to be significantly biased. This makes the development and testing of initialization difficult. When initialized with observations, the model therefore drifts toward their preferred imperfect climatology, leading to biases in the forecasts. Such biases will grow with the length of forecast because of nonlinearities. The development of climate models with better horizontal and vertical resolutions is also a priority for decadal climate prediction, and the important physical mechanisms should be well represented in the model used for decadal prediction. However, while the influence of the tropical oceans on the atmosphere is established, the role of extratropical ocean changes on the atmosphere is unclear. Additionally, decadal climate predictions require the accurate projection of external radiative forcing. At present, dynamical model systems yield some predictability for the SST, but limited predictability for the atmosphere, particularly for the extratropical regions, at the decadal scale. Thus, the study of decadal climate prediction remains in an early stage at present.

The DEMETER system aims to predict the seasonal-to-interannual variability rather than decadal variability (Palmer et al. 2004). Uncertainties in the initial state are represented through an ensemble of nine different ocean initial conditions. This is achieved by creating three different ocean analyses. The CNRM, ECMWF, and UKMO models, with different vertical and horizontal resolutions, have the same ocean and atmosphere initial conditions.

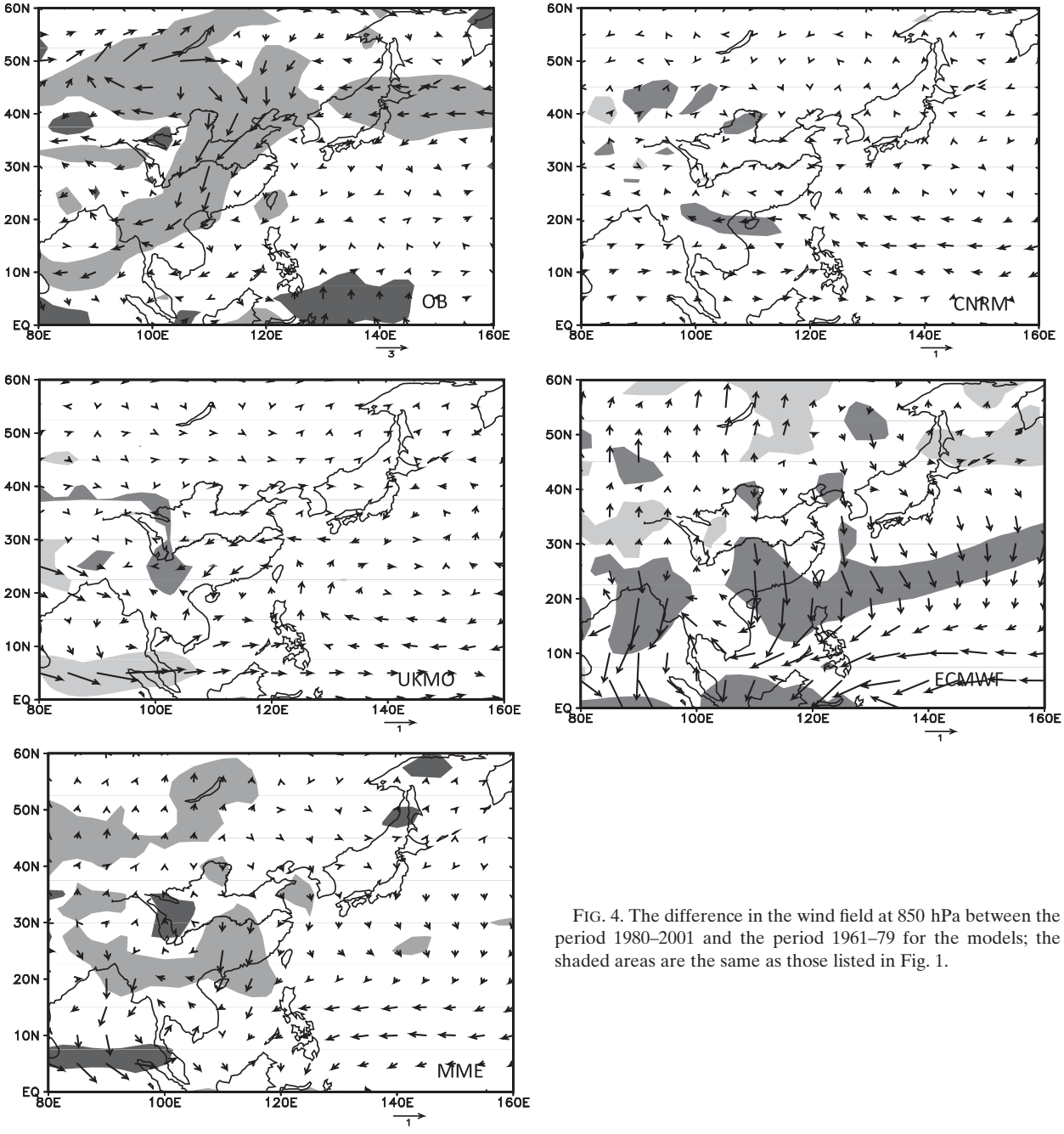

FIG. 4. The difference in the wind field at 850 hPa between the period 1980–2001 and the period 1961–79 for the models; the shaded areas are the same as those listed in Fig. 1.

However, the DY of a variable with an amplified prediction signal can capture the decadal variability and interannual variability. As Fig. 5 has shown, the EASM is significantly and negatively correlated with geopotential height at 500 hPa over East Asia during the 1961–2001 period on interannual and decadal time scales. However, no models can reproduce well the linkage between the EASM and the geopotential height at 500 hPa, Z500, partly due to their poor ability for predicting the decadal variability of the EASM. Meanwhile, the models can reproduce the linkage between the DY of the EASM and the DY of Z500. Particularly, each model shows good performance in the prediction of the western North Pacific circulation, indicating that this circulation pattern is another predictor (x_2) of the EASM.

Therefore, we consider the DY of the EASM derived from direct output sources of the model as a predictor (x_1) for developing prediction scheme I for the EASM. Scheme II was developed containing both x_1 and x_2. The

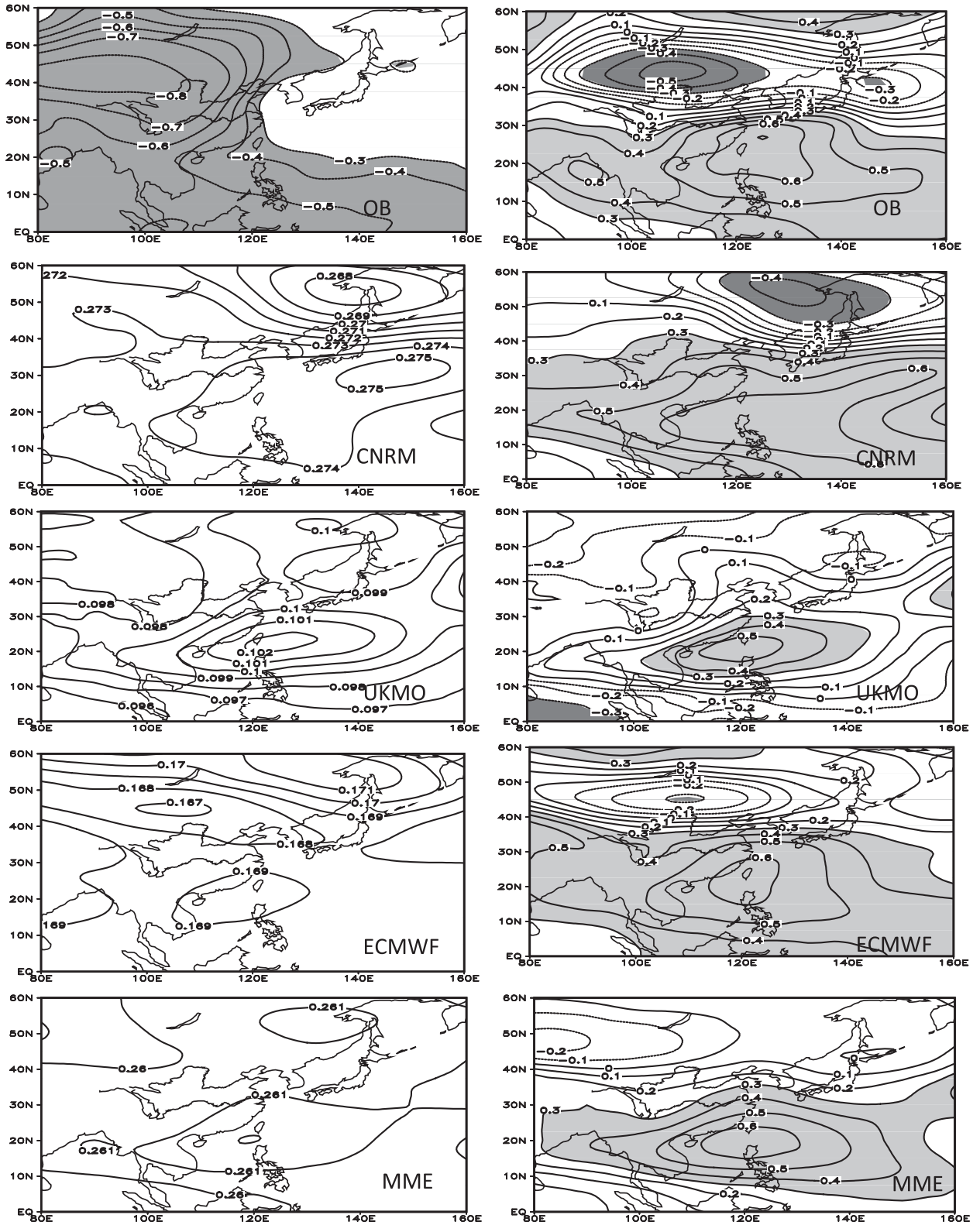

FIG. 5. The correlation coefficient between the EASM index and the geopotential height at 500 hPa for the models (left) in the original form and (right) in the DY form; the shaded areas are the same as those listed in Fig. 1.

TABLE 2. Verification for scheme I for the hindcasts during 1961–2001; boldface values indicate greater than the 95% significance level.

1961–2001	TCC of EASM (DY of EASM)	RMSE (Improvement in RMSE)
CNRM	**0.66 (0.43)**	0.95 (28%)
UKMO	**0.7 (0.49)**	0.9 (30%)
ECMWF	**0.7 (0.5)**	0.9 (−23%)
MME	**0.77 (0.63)**	0.77 (10%)

baseline forecast requires that each of the predictors selected from the output model should be verified based on two considerations. First, each of the models should have good prediction ability for the predictors, as measured by the correlation coefficient between the output model and the observations. Second, the predictors should be significantly correlated with the EASM (Tables 1 and 3 and Fig. 5).

1) SCHEME I

Because the models exhibited reasonable ability in predicting the DY of the EASM rather than the EASM in the original form, prediction scheme I was proposed, in which the predicted EASM was obtained by adding the DY of the EASM derived from the direct outputs of the current-year models to the observed EASM from the previous year. Scheme I for every model was represented by the equation $\hat{y}_i = x_i + y_{i-1}$, where $\hat{y}_i$ denotes the predicted EASM for each of the models, x_i refers to the DY of the EASM derived from the direct output of each model (CNRM, UKMO, ECMWF, and MME), and y_{i-1} represents the observed EASM of the previous year. Thus, we have four schemes for the four models (CNRM, UKMO, ECMWF, and MME).

Figure 5 shows the predicted EASMs for the individual models for the period 1961–2001 that were obtained from the corresponding scheme I. All of the prediction models successfully reproduced the decadal variability of the EASM, which weakened at the end of the 1970s, and properly followed the interannual variability of the EASM. The TCCs of the EASM for the ECMWF, CNRM, UKMO, and MME models were, respectively, 0.7, 0.66, 0.7, and 0.77 for scheme I, and all were above the 95% significance level (compared with 0.7, 0.12, 0.15, and 0.61 for the old scheme, respectively) (Table 2). Compared with each of the old schemes, the percentages of improvement for scheme I in the RMSE were 28%, 30%, and 10% for the CNRM, UKMO, and MME models, respectively, indicating an improved prediction ability for the EASM when scheme I was applied to each of the models. However, the RMSE of the EASM for ECMWF with scheme I (0.89) was larger than the RMSE with the old scheme (0.73), partly due to a large error in 1968 with the new scheme.

Consequently, a more effective scheme II was developed to further improve the predictive ability of the EASM.

2) SCHEME II

Two predictors were used in scheme II. One was the DY of the EASM that was available from the direct outputs of the models. The other predictor represented the circulation associated with the western North Pacific subtropical high in the form of the year-to-year increment because the western North Pacific subtropical high plays an important role in the variability of the East Asian monsoon and monsoon rainfall. As Fig. 5 shows, the increased DY of the 500-hPa geopotential height over the western North Pacific promoted an enhanced DY of the EASM. Importantly, each of the models can show a high level of accuracy in predicting the western North Pacific circulation. Then, we defined x_2 as the area-average DY of the geopotential height at 500 hPa over the region (10°–30°N, 110°–135°E) obtained from the models, with the correlation coefficient between the observed x_2 and the observed EASM being 0.65 for 1961–2001, which exceeds the 99% significant level. The correlation coefficient between the observed x_2 and the simulated x_2 for the CNRM, UKMO, ECMWF and MME results for 1961–2001 were 0.75, 0.71, 0.75, and 0.77, respectively, all of which were above the 99% significant level. In addition, the correlation coefficients between x_2 and the DY of the EASM for the CNRM, UKMO, ECMWF and MME models for 1961–2001 were 0.61, 0.66, 0.59, and 0.65, respectively, exceeding the 99% significant level.

Subsequently, the statistical scheme II for the ECMWF, CNRM, UKMO and MME models was established using the multilinear regression method, in which two predictors (x_1 and x_2) in the form of year-to-year increments were contained. For example, the downscaling prediction scheme II for the CNRM was represented by the two equations

$$\Delta\hat{y}_i(\mathrm{CNRM}) = ax_{1i}(\mathrm{CNRM}) + bx_{2i}(\mathrm{CNRM}), \quad \text{and}$$
$$\hat{y}_i(\mathrm{CNRM}) = \Delta\hat{y}_i(\mathrm{CNRM}) + y_{i-1}(\mathrm{CNRM}),$$

where $\Delta\hat{y}_i$(CNRM) represents the DY of the EASM for the CNRM for one current year, $\hat{y}_i$ (y_i) denotes the prediction (observed) of the EASM in the original form for one current year, and y_{i-1} refers to the observed EASM of the previous year. The variables x_1 and x_2 denote two predictors obtained from the CNRM in the form of the year-by-year increment, whereas a and b

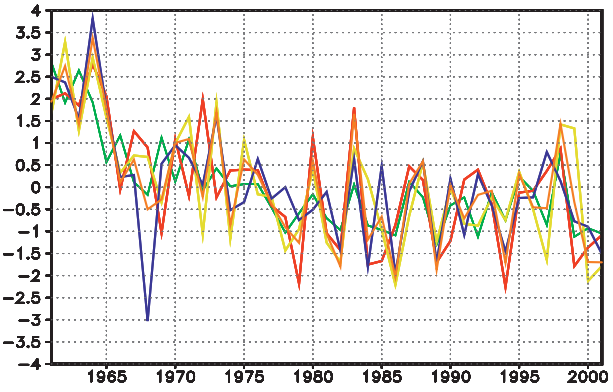

FIG. 6. Verification for scheme I for 1961–2001: observed values (green), and predicted values for CNRM (red), UKMO (yellow), ECMWF (blue), and MME (orange).

represent the regression coefficients. In this way, scheme II was established for each of the models.

A critical part of the prediction scheme was the evaluation of the prediction using independent data, and thus two separate tests were performed to validate scheme II. The first approach was a cross-validation test for the period 1961–2001 (41 yr), and the other used hindcasts for 1986–2001 (16 yr). The TCC and the percentage of improvement in the RMSE measured the prediction ability. In the cross-validation test for 1961–2001 using scheme II, the prediction ability of each of the models (CNRM, UKMO, ECMWF and MME) improved significantly (Fig. 6, Table 3), with the TCCs of the EASM for the CNRM, UKMO, ECMWF, and MME models given as 0.8, 0.85, 0.8, and 0.86, respectively, compared with direct outputs of the models of 0.12, 0.15, 0.71, and 0.61, respectively. Compared with the old scheme, the percentages of improvement in the RMSE of the EASM for the CNRM, UKMO, ECMWF, and MME results for the new scheme II were 54%, 56%, 15%, and 37%, respectively (Table 4). After the downscaling prediction, the models reproduced the variation of the EASM for both the interannual and decadal time scales, which successfully captured the weakened EASM at the end of the 1970s.

We also made a hindcast for 1986–2001 (16 yr) using scheme II (Fig. 8). For example, we used the 1961–85 dataset to forecast the 1986 values, we used the 1961–86 dataset to predict the 1987 values, and we employed the 1961–2000 dataset to predict the 2001 values. In this way, for each of the models, we had 16 hindcast years derived from 16 equations whose coefficients varied slightly with time, suggesting a stable relationship between the two predictors and the EASM. Figure 7 shows that the predicted EASM for each of the models followed the interannual variability of the observed EASM. The

TABLE 3. TCC between the observed DY of the WNP circulation and the modeled DY of the WNP circulation.

Model	Observed, 1965–2001	Observed, 1961–79	Observed, 1980–2010
CNRM	0.74	0.44	0.87
UKMO	0.71	0.48	0.83
ECMWF	0.75	0.53	0.85
MME	0.77	0.52	0.88

correlation coefficient between the downscaling modeled DY of the EASM (EASM) and the observed DY of the EASM (EASM) for 1986–2001 for the CNRM, UKMO, ECMWF, and MME models were 0.92 (0.62), 0.84 (0.72), 0.86 (0.59), and 0.86 (0.82), respectively, exceeding the 95% significance level (Table 5). The simulated and observed EASM results exhibited reasonable agreement both qualitatively and quantitatively during the hindcasts for 1986–2001. Compared with the direct outputs of the models (Fig. 2, Table 1), the percentages of improvement in the RMSE for the CNRM, UKMO, ECMWF, and MME models for scheme II were 56%, 55%, 1%, and 50%, respectively (Tables 3 and 4). Using the interannual increment prediction approach, the predictive ability of CNRM and UKMO improved substantially for seasonal predictions of interannual and decadal variability of the EASM. However, the percentage improvement (1%) of the prediction ability was not remarkable when scheme II was applied to the ECMWF because of the ECMWF's reasonable prediction ability in the seasonal prediction of the EASM for 1986–2001.

In fact, scheme II for each of the models showed the best prediction ability, with higher TCCs and higher percentages of improvement in the RMSE compared with the original direct outputs of the models and scheme I. Notably, when scheme I was applied to the prediction of the EASM, the models for CNRM and UKMO exhibited remarkable prediction ability. Therefore, capturing the decadal and interannual variability of the EASM with a low RMSE and significant TCC was effective when the interannual increment approach was applied for the downscaling prediction for the EASM.

TABLE 4. Verification for scheme II in the cross-validation test during 1961–2001; boldface values are the same as those listed in Table 1.

	TCC of EASM (DY of EASM)	RMSE (Improvement in RMSE)
CNRM	**0.8 (0.6)**	0.6 (54%)
UKMO	**0.85 (0.72)**	0.56 (56%)
ECMWF	**0.8 (0.64)**	0.62 (15%)
MME	**0.86 (0.75)**	0.54 (37%)

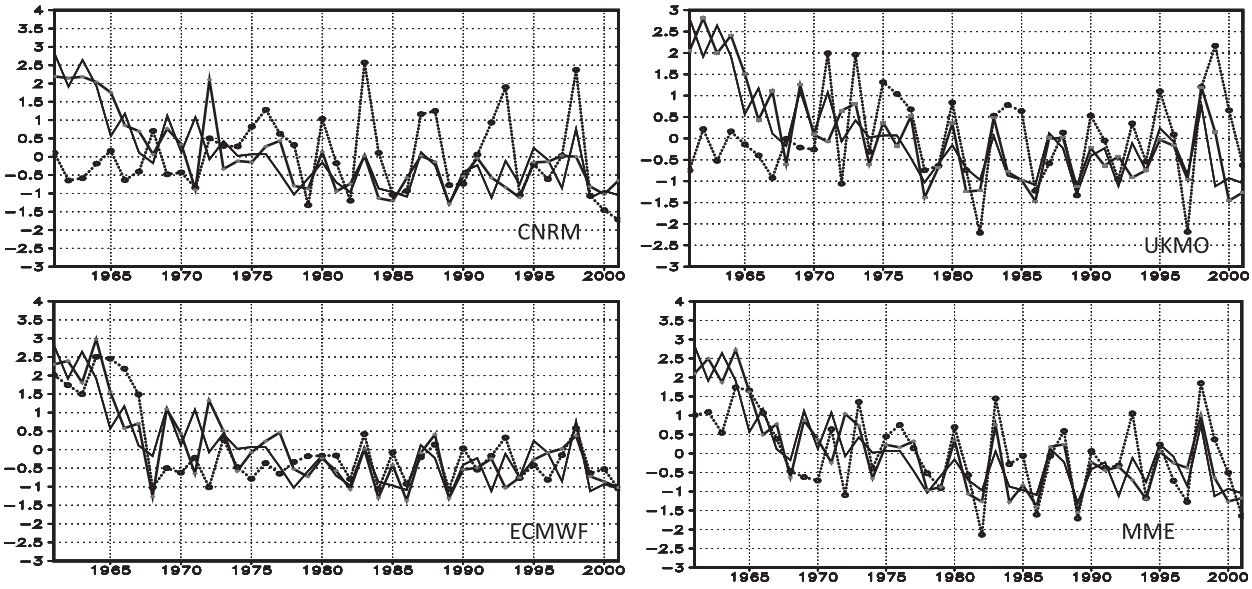

FIG. 7. Verification for scheme II in the cross-validation test for 1961–2001: observed values (solid line), the original model (dashed line with circle), and predicted values (solid line with dot) for (top left) CNRM, (top right) UKMO, (bottom left) ECMWF, and (bottom right) MME.

5. Conclusions

We evaluated the prediction ability of the three DEMETER models (CNRM, UKMO, and ECMWF) and MME in the seasonal prediction of the EASM. The CNRM and UKMO had no prediction ability for the EASM, with an insignificant TCC and a large RMSE due to the inability to reproduce both the weakened EASM at the end of the 1970s and the related changes in the decadal circulations (Figs. 2–5 and Table 1). Therefore, the interannual increment prediction approach was applied to improve the prediction ability of the models because a variable of the interannual increment was able to capture the decadal trend of the variable in the original form. The direct outputs of the models (CNRM, UKMO, ECMWF, and MME) were better able to predict the seasonal variation of the DY of the EASM than the EASM in its original form (Fig. 2b). Therefore, we developed two statistical schemes for each of the models to forecast the EASM using the interannual increment prediction approach. Scheme I for the EASM for every model was proposed, and this approach contained the DY of the EASM as the only predictor; the predicted EASM for every model was obtained by the DY of the EASM derived from the direct output of the model to the observed previous year of the EASM. Scheme I for every model more accurately predicted the EASM than the original model (Fig. 6, Table 2), excluding the ECMWF version. In particular, the TCCs of the CNRM (0.66) and the UKMO (0.7) simulations for the corrected scheme showed an improved prediction ability with scheme I at 28% and 38% for CNRM and UKMO, respectively.

Scheme II contained two predictors derived from the model outputs. One predictor was the DY of the EASM, and the other was the DY of circulation related to the western North Pacific subtropical high. Through the cross-validation test for 1961–2001 (41 yr) (Fig. 7, Table 2) and the hindcast for 1985–2001 (Fig. 8 and Tables 4 and 5), the new statistical prediction scheme II largely improved the prediction ability of each model, particularly for CNRM and UKMO. Therefore, the interannual increment prediction approach was highly effective in improving the seasonal climate prediction ability for the dynamical or statistical model, as the DY of a variable can capture the TBO and variation of the interannual and decadal time scales.

What are reasons for the limited improvement in the prediction of EASM in ECMWF with the DY method? It might be that ECMWF has the best ability to predict the EASM among the models, as it can reasonably reproduce the decadal variability of the EASM (see

TABLE 5. Verification for scheme II for the hindcasts during 1986–2001; boldface values are the same as those listed in Table 1.

1986–2001	TCC of EASM (DY of EASM)	RMSE (Improvement In RMSE)
CNRM	**0.62 (0.72)**	0.45 (56%)
UKMO	**0.39 (0.56)**	0.48 (55%)
ECMWF	**0.59 (0.62)**	0.48 (1%)
MME	**0.68 (0.76)**	0.36 (50%)

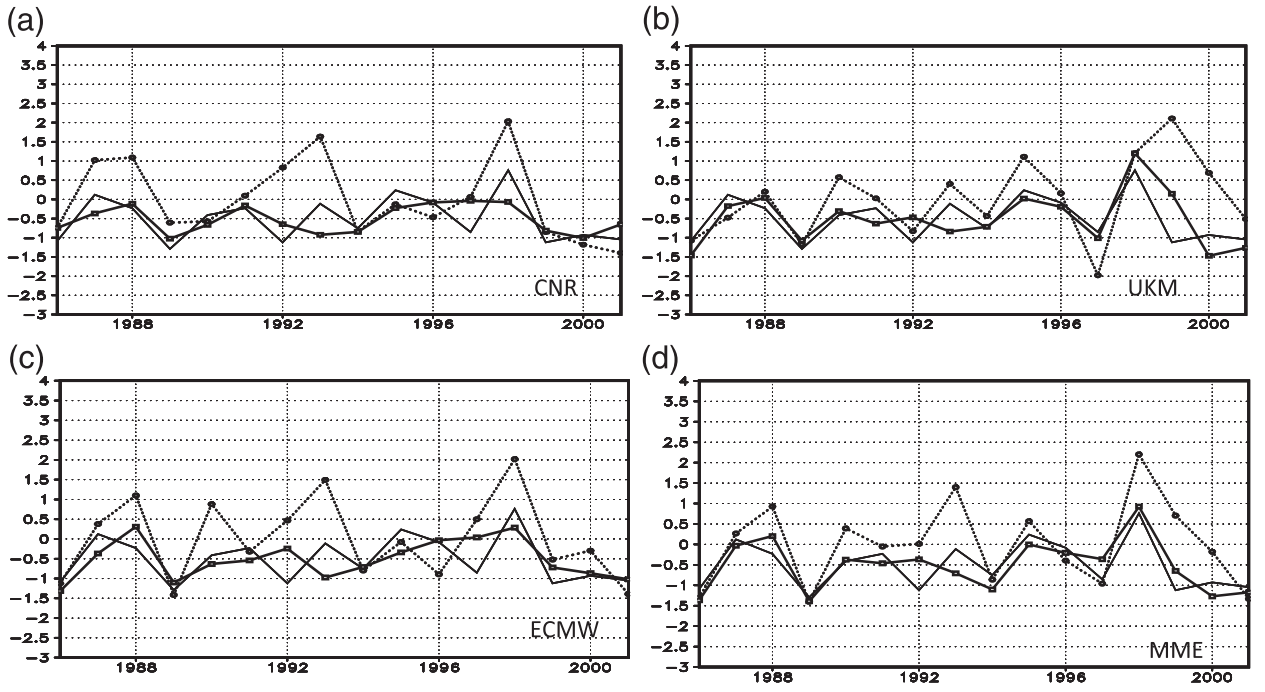

FIG. 8. Verification for scheme II with the hindcasts for 1986–2001: observed values (solid line), the original model (dashed line with circle), and predicted values (solid line with dot) for (top left) CNRM, (top right) UKMO, (bottom left) ECMWF, and (bottom right) MME.

Table 1), such that the TCC of the EASM (0.71) is better than the TCC of the DY of the EASM (0.5) during the 1961–2001 period (Table 1). Additionally, improved prediction ability will depend on the models' prediction abilities for two factors (i.e., DY of the EASM and DY of WNP circulation). Therefore, improved prediction ability for the ECMWF using the DY method is limited.

We tested the neural network method for the prediction here with the same set of predictors. The results are listed in Table 6. The multilinear regression has better prediction skill than does the neural network, although the neural network model can also greatly improve the prediction skill of the EASMI for all models except for MME.

Acknowledgments. The authors would like to thank two reviewers for helpful comments that improved this paper. This research was jointly supported by the Special Fund for the Basic Research Program of China (Grant 2010CB950304), the National Nature Science Foundation of China (Grant 41175071), the Public Welfare Industry (Meteorology) (Grant GYHY200906018), and the Knowledge Innovation Program of the Chinese Academy of Sciences (Grant KZCX2-YW-QN202).

APPENDIX

The DY Method

Traditionally, the anomaly of a variable relative to its climatology is used as the object of short-term climate prediction. However, because the decadal variability of the climate causes difficulties for seasonal climate prediction, the traditional climate predictions are not able to consider climate observations from previous years and the feature of the quasi-biennial oscillation. We

TABLE 6. Comparison of the neural network method with multilinear regression (ML).

	Correlation		RMSE		Improvement In RMSE
Model	Original	BP_Neural(ML)	Original	BP_Neural(ML)	BP_Neural(ML)
CNRM	0.12	0.62 (0.8)	1.32	0.91 (0.6)	31% (54%)
UKMO	0.15	0.79 (0.85)	1.29	0.71 (0.56)	45% (56%)
ECMWF	0.71	0.79 (0.8)	0.73	0.65 (0.62)	11% (15%)
MME	0.61	0.86 (0.86)	0.86	0.86 (0.54)	0% (37%)

propose a year-to-year increment approach or DY method (i.e., difference in any variable between the current year and the previous year), using the interannual increment of a variable as the prediction object (Fan et al. 2008). We apply this method using three steps:

1) We defined the difference in any variable y between the current year (y_i) and the previous year (y_{i-1}); then, $dy_i = y_i - y_{i-1}$.
2) A statistical forecast model for predicting dy_i was established, and the predictors were in the form of the year-to-year increment.
3) The predicted $\hat{y}_i$ was then derived as the sum of the predicted dy_i from the current year and observed y_{i-1} from the preceding year, which is expressed by $\hat{y}_i = dy_i + y_{i-1}$.

There are several advantages of this year-to-year increment or DY method. First, the rationale for the year-to-year increment approach might arise from the existence of the tropospheric biennial oscillation (TBO) during the Asian monsoon, ENSO, rainfall, and temperature over east China, etc. The interannual increment of a variable reflects the TBO to amplify the prediction signal and makes good use of the climate observations from the previous year (Wang et al. 2010). If we consider the TBO feature in climate variables, and f_i (f_{i-1}) represents the anomaly of a variable in the current year (previous year), such that $f_i = c + p_i$ and $f_{i-1} = -c + p_{i-1}$, in which p and p_{i-1} represent a disturbance of f, then $f_i \approx c$ and $\Delta f_i = f_i - f_{i-1} \approx 2c$. These relationships suggest that the amplitude of a variable in the form of the year-to-year increment is twice that in the form of an anomaly, and the prediction signal can be amplified. Second, the DY method can capture the interannual and decadal variability of the climate. The DY of Y can remove the decadal trend of the climate, but the accumulation of the DY of Y can reproduce the decadal trend.

REFERENCES

Ding, Y., and J. C. L. Chan, 2005: The East Asian summer monsoon: An overview. *Meteor. Atmos. Phys.,* **89,** 117–142.

Fan, K., 2009: Predicting winter surface air temperature in northeast China. *Atmos. Oceanic Sci. Lett.,* **2,** 14–17.

——, 2010: A prediction model for Atlantic named storm frequency using a year-by-year increment approach. *Wea. Forecasting,* **25,** 1842–1851.

——, and H. J. Wang, 2006: Interannual variability of Antarctic Oscillation and its influence on East Asian climate during boreal winter and spring. *Sci. China,* **49D,** 554–560.

——, and ——, 2009: A new approach to forecasting typhoon frequency over the western North Pacific. *Wea. Forecasting,* **24,** 974–978.

——, ——, and Y. J. Choi, 2008: A physically-based statistical forecast model for the middle-lower reaches of the Yangtze River valley summer rainfall. *Chin. Sci. Bull.,* **53,** 602–609.

——, M. J. Lin, and Y. Z. Gao, 2009: Forecasting the summer rainfall in north China using the year-to-year increment approach. *Sci. China,* **52D,** 532–539.

Gao, X. J., J. S. Pal, and F. Giorgi, 2006: Projected changes in mean and extreme precipitation over the Mediterranean region from a high resolution double nested RCM simulation. *Geophys. Res. Lett.,* **33,** L03706, doi:10.1029/2005GL024954.

Ju, L. X., H. J. Wang, and D. B. Jiang, 2007: Simulation of the Last Glacial Maximum climate over East Asia. *Palaeogeogr. Palaeoclimatol. Palaeoecol.,* **248,** 376–390.

Kang, I.-S., and Coauthors, 2002: Intercomparison of the climatological variations of Asian summer monsoon precipitation simulated by 10 GCMs. *Climate Dyn.,* **19,** 383–395, doi:10.1007/s00382-002-0245-9.

Keenlyside, N. S., M. Latif, J. Jungclaus, L. Kornblueh, and E. Roeckner, 2008: Advancing decadal-scale climate prediction in North Atlantic sector. *Nature,* **453,** 84–88.

Krishnamurti, T. N., C. M. Kishtawal1, T. E. LaRow, D. R. Bachiochi, Z. Zhang, C. E. Williford, S. Gadgil, and S. Surendran, 1999: Improved weather and seasonal climate forecasts from multimodel superensemble. *Science,* **285,** 1548, doi:10.1126/science.285.5433.1548.

Lang, X. M., and H. J. Wang, 2010: Improving extraseasonal summer rainfall prediction by merging information from GCMs and observations. *Wea. Forecasting,* **25,** 1263–1274.

Liu, Y., K. Fan, and H. J. Wang, 2011: Statistical downscaling prediction of summer precipitation in southeastern China. *Atmos. Oceanic Sci. Lett.,* **4,** 173–180.

Meehl, G. A., and Coauthors, 2009: Decadal prediction—Can it be skillful? *Bull. Amer. Meteor. Soc.,* **90,** 1467–1485.

Murphy, J., and Coauthors, 2010: Towards prediction of decadal climate variability and change. *Proc. Environ. Sci.,* **1,** 287–304.

Palmer, T. N., and Coauthors, 2004: Development of a European Multimodel Ensemble System for Seasonal-to-Interannual Prediction (DEMETER). *Bull. Amer. Meteor. Soc.,* **85,** 853–872.

Tao, S. Y., and L. X. Chen, 1987: A review of recent research on the East Asian monsoon in China. *Monsoon Meteorology,* C. P. Chang, Ed., Oxford University Press, 60–92.

Wang, H. J., 2000: The interannual variability of the East Asian monsoon and its relationship with SST in a coupled atmosphere–ocean–land climate model. *Adv. Atmos. Sci.,* **17,** 31–47.

——, 2001: The weakening of the Asian monsoon circulation after the end of 1970's. *Adv. Atmos. Sci.,* **18,** 376–386.

——, 2002: Instability of the East Asian summer monsoon–ENSO relations. *Adv. Atmos. Sci.,* **19,** 1–11.

——, and K. Fan, 2005: Central-north China precipitation as reconstructed from the Qing dynasty: Signal of the Antarctic atmospheric oscillation. *Geophys. Res. Lett.,* **32,** L24705, doi:10.1029/2005GL024562.

——, and ——, 2009: A new scheme for improving the seasonal prediction of summer precipitation anomalies. *Wea. Forecasting,* **24,** 548–554.

——, G. Q. Zhou, and Y. Zhao, 2000: An effective method for correcting the seasonal–interannual prediction of summer climate anomaly. *Adv. Atmos. Sci.,* **17,** 234–240.

——, Y. Zhang, and X. M. Lang, 2010: On the predictand of short-term climate prediction (in Chinese). *Climatic Environ. Res.,* **15,** 225–228.

Wilby, R. L., and T. M. L. Wigley, 1997: Downscaling general circulation model output: A review of methods and limitations. *Prog. Phys. Geogr.,* **21,** 530–548.

——, ——, D. Conway, P. D. Jones, B. C. Hewitson, J. Main, and D. S. Wilks, 1998: Statistical downscaling of general circulation model output: A comparison of method. *Water Resour. Res.,* **34,** 2995–3008.

Yang, S., Z. Q. Zhang, V. E. Kousky, R. W. Higgins, S.-H. Yoo, J. Liang, and Y. Fan, 2008: Simulations and seasonal prediction of the Asian summer monsoon in the NCEP Climate Forecast System. *J. Climate,* **21,** 3755–3775.

Zhou, B. T., and H. J. Wang, 2006: Relationship between the boreal spring Hadley circulation and the summer precipitation in the Yangtze River valley. *J. Geophys. Res.,* **111,** D16109, doi:10.1029/2005JD0070006.

Zhu, Y. L., H. J. Wang, W. Zhou, and J. Ma, 2011: Recent changes in the summer precipitation pattern in east China and the background circulation. *Climate Dyn.,* **36,** 1463–1473, doi:10.1007/s00382-010-0852-9.